Biochimica et Biophysica Acta 1827 (2013) 723–729

Contents lists available at SciVerse ScienceDirect

Biochimica et Biophysica Acta

journal homepage: www.elsevier.com/locate/bbabio

Light harvesting complexes of *Chromera velia*, photosynthetic relative of apicomplexan parasites

Josef Tichy [a,b], Zdenko Gardian [a,b], David Bina [a,b], Peter Konik [a], Radek Litvin [a,b], Miroslava Herbstova [a,b], Arnab Pain [c], Frantisek Vacha [a,b,*]

[a] Faculty of Science, University of South Bohemia, Branisovska 31, 37005 Ceske Budejovice, Czech Republic
[b] Institute of Plant Molecular Biology, Biology Centre ASCR, Branisovska 31, 37005 Ceske Budejovice, Czech Republic
[c] Computational Bioscience Research Center, King Abdullah University of Science and Technology, Thuwal 23955-6900, Saudi Arabia

ARTICLE INFO

Article history:
Received 19 October 2012
Received in revised form 31 January 2013
Accepted 5 February 2013
Available online 18 February 2013

Keywords:
Chromera velia
FCP
LHCr
Circular dichroism
Photosystem I
Electron microscopy

ABSTRACT

The structure and composition of the light harvesting complexes from the unicellular alga *Chromera velia* were studied by means of optical spectroscopy, biochemical and electron microscopy methods. Two different types of antennae systems were identified. One exhibited a molecular weight (18–19 kDa) similar to FCP (fucoxanthin chlorophyll protein) complexes from diatoms, however, single particle analysis and circular dichroism spectroscopy indicated similarity of this structure to the recently characterized XLH antenna of xanthophytes. In light of these data we denote this antenna complex CLH, for "Chromera Light Harvesting" complex. The other system was identified as the photosystem I with bound Light Harvesting Complexes (PSI–LHCr) related to the red algae LHCI antennae. The result of this study is the finding that *C. velia*, when grown in natural light conditions, possesses light harvesting antennae typically found in two different, evolutionary distant, groups of photosynthetic organisms.

1. Introduction

Chromera velia (Chromerida; Alveolata; Chromalveolata; Eukaryota) is a photosynthetic unicellular alga that was isolated as a supposed symbiont of coral *Plesiastrea versipora* from the eastern coast of Australia [1]. *C. velia* with its recently described close relative *Vitrella brassicaformis* are the only known photosynthetic relatives of apicomplexans [1,2], that are strict heterotrophs or parasites. Apicomplexans contain an unpigmented chloroplast remnant called apicoplast which has lost all properties necessary for photosynthesis [3]. According to the Chromalveolate hypothesis [4], apicomplexan parasites together with heterokonts, haptophytes, cryptophytes and dinoflagellates have acquired their chloroplast through secondary endosymbiosis of a free-living photosynthetic red alga [5,6]. Due to substantial differences of apicoplasts and the above mentioned algae genomes, it has not been possible to perform a reliable comparison study before the discovery of *C. velia*.

C. velia has three life stages — coccoid, cystic and flagellate. The coccoid form containing several chloroplasts is predominant in the stationary phase whilst transformation from a coccoid into a flagellate form occurs in an exponentially growing culture [7].

Each cell of *C. velia* has one or two golden-brown cone-shaped chloroplast/s bound by four membranes, with thylakoids in a stack of three or more. *C. velia* contains chlorophyll (Chl) *a*, violaxanthin and a novel isofucoxanthin-like carotenoid as major components, and β-carotene as a minor component. *C. velia* was shown to possess a functioning xanthophyll cycle as a protection against excess irradiance. As a consequence, large amount of zeaxanthin can be detected in stressed cells [8].

Except for Chl *a*, no other chlorophylls have been detected, apart from trace amount of derivate of Chl *c*, magnesium-divinyl-pheoporphyrin a5 monomethyl ester (MgDVP). The novel carotenoid pigment (isofucoxanthin-like) was identified by Moore and coworkers [1] using mass spectrometry analysis as an isomer of isofucoxanthin, although the absorbance spectral data did not support this assignment. The absorption maximum of isofucoxanthin in methanol is 454 nm, however, the novel carotenoid has its maximum in methanol at 467.5 nm [1]. The pigment analysis of *C. velia* obtained by HPLC demonstrates different characteristics compared to its sister organism

Abbreviations: BLAST, the basic local alignment search tool; Chl, chlorophyll; CD, circular dichroism; DDM, *n*-dodecyl β-D-maltoside; FCP, fucoxanthin chlorophyll protein complexes; HPLC, high performance liquid chromatography; LHC, light harvesting complex; LHCr, red alga like light harvesting complex; MES, 2-Morpholinoethanesulfonic acid; MgDVP, magnesium-divinyl-pheo-porphyrin a5 monomethyl ester; MS, mass spectrophotometry; PDA, photodiode array detector; PS, photosystem; Q-TOF MS, quadrupole time of flight mass spectrometer; SDS-PAGE, sodium dodecyl sulphate-polyacrylamide gel electrophoresis; TEM, transmission electron microscopy; XLH, xanthophytes' light harvesting antenna complex

* Corresponding author at: Faculty of Science, University of South Bohemia, Branisovska 31, 37005 Ceske Budejovice, Czech Republic. Tel.: +420 389 022 244.
E-mail address: vacha@jcu.cz (F. Vacha).

0005-2728/$ – see front matter © 2013 Elsevier B.V. All rights reserved.
http://dx.doi.org/10.1016/j.bbabio.2013.02.002

V. brassicaformis, where the pigment composition is the same as in *Nannochloropsis limnetica* (Eustigmatophyceae, Heterokonta) [2,9].

Chloroplast genes of *C. velia* have been found to be related to a red algal chloroplast [10]. However, protein sequence analyses of light harvesting complexes (LHCs) demonstrated there to be multiple variants of evolutionary pathways [11]. According to this study, *C. velia* contains 23 peptide sequences of LHCs within its nuclear genome. The majority of them (17 of the 23) form a group with a sister relationship to fucoxanthin chlorophyl *a*/*c*-binding LHCs (FCPs) of Chl *c* containing algae, including diatoms, brown algae and dinoflagellates [12], but separated from the main algal LHC groups. The rest of the LHC peptide sequences were characterized by phylogenetic analysis as a part of one of three smaller groups: (a) three sequences were related to the LHCr, red algae-like LHC from diatoms; (b) a single sequence from the LI818 protein group of stress-related proteins found both in green algae and chromalveolates [13] and (c) two sequences positioned on two separate branches with the antenna proteins of the xanthophyte *Vaucheria litorea* (yellow-green alga).

The present study describes the first isolation of the light harvesting pigment–protein complexes of *C. velia*. Two different antenna complexes were identified, showing sequential similarity to FCP antenna of diatoms and the photosystem I with bound Light Harvesting Complex (PSI–LHCr) of the red algae, respectively. Biochemical, spectroscopic and electron-microscopic characterization of these pigment–protein complexes is presented.

2. Materials and methods

2.1. Culture and growth conditions

Cells of *C. velia* were grown in 5 l Erlenmeyer flasks at 27 °C in modified f2 saline medium for diatoms [14] and bubbled with filtered air. The culture was irradiated by common daylight with the intensity around 100 μmol photons m^{-2} s^{-1}. Cells were harvested at stationary phase (1 month old culture) by centrifugation at 4000 ×*g* for 5 min, then resuspended and washed twice by MES buffer (50 mM MES, pH 6.5; 5 mM $CaCl_2$; 10 mM NaCl) and stored at −70 °C.

The cells were harvested in the stationary phase to minimize the presence of the flagellate form in the culture [7], and to preserve the uniformity of the culture as much as possible.

2.2. Thylakoid membrane isolation

Cells were twice treated by freeze–thaw cycle to facilitate their breakage. Cells were then broken by several passages through an EmulsiFlex-C5 High Pressure cell disrupter (Avestin Inc., Canada) at a pressure of 100–150 MPa, whilst keeping the apparatus refrigerated on ice in the dark. The unbroken cells were removed by centrifugation for 10 min at 500 ×*g*. The supernatant was then centrifuged for 45 min at 60,000 ×*g* to pellet thylakoid membranes without pelleting cell envelope fragments. Membranes were resuspended in MES buffer (50 mM MES, pH 6.5; 5 mM $CaCl_2$; 10 mM NaCl) and solubilized with 5% *n*-dodecyl β-D-maltoside at chlorophyll concentration of 1 mg ml^{-1} for 45 min in the dark on ice. The unsolubilized material was removed by centrifugation for 20 min at 30,000 ×*g* and the supernatant was loaded onto a fresh 0–1.0 M continuous sucrose density gradient prepared by freezing and thawing the centrifuge tubes filled with 0.55 M sucrose in DDM/MES buffer (50 mM MES; 5 mM $CaCl_2$; 10 mM NaCl; pH 6.5 and 0.02% *n*-dodecyl β-D-maltoside). The following centrifugation was carried out at 4 °C using a SW-40 swing-out rotor (Beckman Coulter) at 150,000 ×*g* for 16 h. Zones resolved by the sucrose density gradient were further desalted by a gel filtration using Sephadex G-25 column (Amersham Biosciences, Sweden) and used immediately or stored in MES buffer at −70 °C.

2.3. Absorption, fluorescence and circular dichroism spectroscopy

Chlorophyll concentration was determined spectroscopically in 80% acetone according to Lichtenthaler [15]. Room temperature absorption spectra were recorded with a UV300 spectrophotometer (Spectronic Unicam, Cambridge, UK).

Low temperature fluorescence emission spectra were recorded at 77 K using a Spex Fluorolog-2 spectrofluorometer (Jobin Yvon, Edison, NJ, USA) in the spectral range of 620–780 nm (slit width 2 nm) with an excitation wavelength of 435 nm (slit width 3.2 nm). The chlorophyll concentration of the samples used for measurements was adjusted to 10 μg (Chl *a* ml^{-1}).

Circular dichroism (CD) spectra were recorded with a Jasco J-715 spectropolarimeter (slit width 2 nm). Prior to the CD measurements, samples were further purified by applying the zone from a sucrose density gradient to a Superdex 200 GL 10/300 gel-filtration column (GE Healthcare) equilibrated with DDM/MES buffer (50 mM MES; 5 mM $CaCl_2$; 10 mM NaCl; pH 6.5 and 0.02% *n*-dodecyl β-D-maltoside).

2.4. Pigment composition

C. velia pigments were analyzed by high-performance liquid chromatography (HPLC) consisting of a Pump Controller Delta 600, Autosampler 2707 injection system and a PDA 2996 detector (Waters, USA). Pigments were separated on a reverse phase Sunfire™ C8 column (4.6×250 mm, 5 μm, silica-based, end-capped, Waters, USA) using a tertiary solvent system (0–1 min 100% A, followed by a linear gradient until the 11th min to 100% B, and then until the 13th min to 100% C; solution A consisted of 50% methanol, 25% acetonitrile and 25% water, solution B was 100% methanol and solution C was 80% methanol with 20% hexane). Flow rate was 1 ml min^{-1}. The photosynthetic pigment molar ratios were estimated from areas under the chromatograph peaks displayed at wavelengths corresponding to the particular extinction coefficients. The molar extinction coefficient ε (dm^3 $mmol^{-1}$ cm^{-1}) was 71.43 for Chl *a* at 665 nm [16], 144 for violaxanthin at 439 nm, 134 for zeaxanthin at 472 nm, 139 for β-carotene at 453 nm [17]. As the extinction coefficient for the isofucoxanthin-like carotenoid has not yet been determined, the coefficient of fucoxanthin of 109 (given at 453 nm in Ref. [17]) was used for the absorbance measured in the maximum at 467.5 nm [1].

2.5. Protein composition

C. velia protein composition was determined by SDS-PAGE using a precast 12% polyacrylamide SDS gel (C.B.S. Scientific) and stained with Coomassie Brilliant Blue or by silver stain. Apparent molecular weights were estimated by co-electrophoresis of a low molecular weight protein standard (Fermentas).

2.6. TEM microscopy

Freshly prepared photosynthetic complexes were immediately used for transmission electron microscopy (TEM). Specimens were placed on glow-discharged carbon-coated copper grids and negatively stained with 2% uranyl acetate, visualized by TEM and processed by image analysis. TEM was performed using a JEOL 1010 transmission electron microscope (JEOL, Japan) at 80 kV and 60,000× magnification. Micrographs were digitized with a pixel size corresponding to 5.1 Å at the specimen level. Image analyses were carried out using the Spider and Web software package [18]. Manually selected projections were rotationally and translationally aligned, and treated by multivariate statistical analysis in combination with classification procedure [19,20]. Classes from each of the subsets were used for the refinement of alignments and subsequent classifications. For the final sum, the best of the class members were summed using a cross-correlation coefficient of the alignment procedure as a quality parameter [19].

2.7. MS/MS analysis

Gel slices were prepared for tryptic digestion and subsequently subjected to in-gel digestion using Proteomic Grade Trypsin (Sigma) according to the manufacturers' instructions. Gel slices were de-stained in 200 μl of 200 mM ammonium bicarbonate in 40% (v/v) acetonitrile at 37 °C. After 30 min the solution was discarded and the procedure was repeated. Gel slices were then dried for approx. 20 min in a speedvac. The slices were then left to soak the solution of 20 μg ml^{-1} proteomic grade trypsin (Sigma) in 40 mM ammonium bicarbonate in 9% (v/v) acetonitrile for 45 min at 4 °C. The solution was then discarded and 30 μl of 40 mM ammonium bicarbonate in 9% (v/v) acetonitrile was added to the slices. The slices were then incubated for 12 h at 37 °C. Peptides from the solution were isolated through the use of ZipTip C18 pipette tips (Millipore). The tips were wetted by 100% acetonitrile (3 times 10 μl) and equilibrated by 1% (v/v) formic acid (3 times 10 μl). Peptides were then allowed to bind to the C18 matrix by aspirating the sample solution 10 times through the equilibrated tip. The tip was then aspirated 10 times with 1% (v/v) formic acid. Peptides were then eluted by using 20 μl of 50% (v/v) acetonitrile in 1% formic acid. MS analysis was performed on a NanoAcquity UPLC (Waters) on-line coupled to an ESI Q-TOF Premier Mass spectrometer (Waters). A sample volume of 1 μl was diluted in 3% (v/v) acetonitrile in water with 0.1% (v/v) formic acid and separated by reverse phase chromatography on a BEH300 C18 analytical column (75 μm i.d. × 150 mm length, particle size 1.7 μm, reverse-phase; Waters, UK). A linear gradient from initial conditions of 3% (v/v) B to final conditions of 40% (v/v) B in solvent A) was applied with a flow rate of 0.4 μl min^{-1} in 30 min (solvent A was 0.1% (v/v) formic acid in water and solvent B was 0.1% (v/v) formic acid in acetonitrile). Peptides eluted from the column were introduced directly into a Q-TOF mass spectrometer. Precursor ion spectra were acquired with a collision energy of 5 V and fragment ion spectra with a collision energy of 20–35 V ramp. Peptide and fragment spectra were acquired with 2 ppm and 5 ppm tolerance, respectively. Raw data were processed and resulting peptides were subjected to a database search using PLGS2.3 software (Waters) and an in-house predicted Chromera protein database, currently available in-house as a part of the *C. velia* genome sequencing project (the sequences of identified peptides are given in the Supplementary data Section 2) and from publicly available transcriptome sequencing datasets on *C. velia* [21]. Additional peptide analysis was performed using BLASTp tool with default values [22].

3. Results and discussion

Thylakoid membranes solubilized with *n*-dodecyl β-D-maltoside (DDM) were separated by sucrose density gradient centrifugation into four zones [Fig. 1A, the original photograph is seen in Supplementary Fig. 1]. Zones one, three and four were green whilst the second zone was brown. All zones were characterized by their absorption and fluorescence spectra as well as pigment and protein composition.

The absorption spectra of the sucrose density gradient zones [Supplementary Fig. 2] differed slightly in the positions of their chlorophyll Q_y band maxima being at 671, 674, 673 and 677 nm, respectively. However, the main differences were visible in the region of carotenoid absorption. Zones three and four were similar in their carotenoid absorption with maxima around 490 nm, whilst zones one and two had a broad shoulder in the area of 500–550 nm with a sharp peak at ~480 nm.

Results of the HPLC analysis are presented in Table 1. Each zone contained chlorophyll *a* with a retention time of 21.9 min, and two carotenoids, violaxanthin and the isofucoxanthin-like carotenoid, with retention times of 16 and 17 min, respectively. In zones three and four the isofucoxanthin-like carotenoid was present only in a small amount [Table 1]. Besides these major pigments, the first, third and fourth zones contained small amounts of β-carotene. The high content of isofucoxanthin-like carotenoid in first and second zones corresponds well with the longwave carotenoid absorption in these zones, especially zone two.

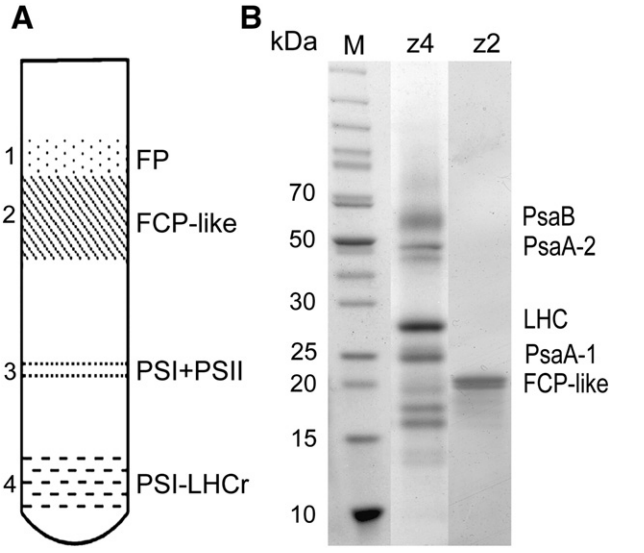

Fig. 1. (A) Representation of the sucrose density gradient zones acquired by ultracentrifugation on a linear gradient of 0 to 1.0 M sucrose. Thylakoids of *C. velia* were solubilized with *n*-dodecyl β-D-maltoside (0.05 g DDM per 1 mg of Chl). (B) SDS-PAGE analysis of pigment–protein complexes of *C. velia* fractionated by sucrose density gradient. Lane (z4) represents zone 4, (z2) zone 2, resolved after sucrose density gradient ultracentrifugation of thylakoid membranes solubilized with DDM. An amount corresponding to 5 μg of Chl was loaded per lane. Molecular weight markers (in kDa) are indicated on left.

The SDS-PAGE of the first zone did not show any proteins, thus, it is most likely composed of free pigments. Since these come most probably from degraded pigment–protein complexes, the pigment composition of this zone is a mixture of pigments found in zones 2–4, thus both fucoxanthin and violaxanthin associated with antennae complexes and β-carotene found in photosystems. The SDS-PAGE of zone two and zone four contained photosynthetic proteins that were identified as constituents of FCP-like antennae and PSI–LHCr complexes, respectively, as based on further analyses (see below). Therefore, in the following sections the second and fourth zones are referred to as the FCP-like zone and the PSI–LHCr zone, respectively. The faint third zone contained mostly a mixture of PSI and PSII protein complexes. The yield of this zone varied among preparations according to the rate of the cells' breakage, solubilization process and the amount of loaded sample. In some cases zone 3 was barely visible and an amount of the isolated complexes was close to a detection limit, hence preventing reliable analysis. Despite these difficulties, PSII was successfully identified in zone 3, [for details see Supplementary Fig. 3].

3.1. FCP-like zone

The second zone contained proteins with a molecular mass between 15 and 20 kDa and a strong double band at 18 and 19 kDa

Table 1
Pigment content relative to chlorophyll *a* (%) of zones from the sucrose density gradient and whole cells of *C. velia*.

Zone	Chlorophyll *a*	Isofucoxanthin-like carotenoid	Violaxanthin	β-carotene
1	100	29	14	1
2	100	37	11	0
3	100	2	1	3
4	100	3	16	4
Whole cells	100	21	14	1

[Fig. 1]. This corresponds to a double band previously identified as FCP apoproteins in diatoms [23–26].

The 18 and 19 kDa bands were in-gel trypsin digested and sequenced by mass spectrometry for closer identification. The resulting peptides were searched against an in-house created species-specific *Chromera* protein database (Computational Bioscience Research Center, King Abdullah U.), sequences of the identified proteins are presented in the Supplementary data, Section 2.a. The database search yielded a positive identification of a "Putative fucoxanthin chlorophyll *a*/*c* binding protein (CveliaI_19753.t1)" with 4 identified peptides out of 9, with sequence coverage of 48.8%. The amino acid sequence of the "Putative fucoxanthin chlorophyll *a*/*c* binding protein (CveliaI_19753.t1)" was then subjected to a BLASTp search, which showed a high level similarity with the LHC family of FCP proteins. Our sequence matched exactly the sequence presented by Pan et al. [11], annotated as CV1 contig 347. The analysis presented in the cited work placed this antenna protein within the main, FCP-like, group of *C. velia* LHCs, in agreement with our result.

The fluorescence emission spectrum of zone 2, measured at 77 K, exhibited a single peak with a shape characteristic of Chl *a* emission, with maximum at 687 nm [Fig. 2]. Such emission spectra are consistent with the spectra of FCP antennae [25,27,28].

Purified complexes were visualized by electron microscopy. A quantity of 6400 particles was manually selected from 48 micrographs [Supplementary Fig. 4a] and processed by image analysis. After the classification steps, selected photosynthetic complexes were decomposed into 8 classes, which were divided into 2 groups of particles as shown in Fig. 3A–B. The first group represents a roughly circular particle, approximately 8 nm in diameter [Fig. 3A], whilst the second group [Fig. 3B] corresponds to a larger, ellipsoidal particle approximately 18 nm long and 15 nm wide. In our interpretation, and in line with both FCP-type and higher plant LHCII complexes that have been shown to assemble into trimers and higher oligomers e.g. [24,25,29–31], our smaller particle likely appears as a trimer and the larger particle as an oligomer of FCP-like proteins. The dimension of the smaller 8 nm particle corresponds very well to the size of the LHCII trimer as inferred from the available 3D structures obtained using electron and X-ray crystallography [32,33] as well as single particle analyses [31]. On the other hand, although the apparent cross-sectional area of the larger particle represents about 4 times the area of the trimer, there does not seem to be a straightforward way to assemble the oligomer by simple rearrangement of the trimers in a manner observed in higher plant LHCII [32] and diatom FCP [29].

Interestingly, the two forms of the FCP-like antenna from *C. velia* presented here matched almost exactly the shape and dimensions of complexes isolated earlier from the xanthophyte *Xanthonema debile*

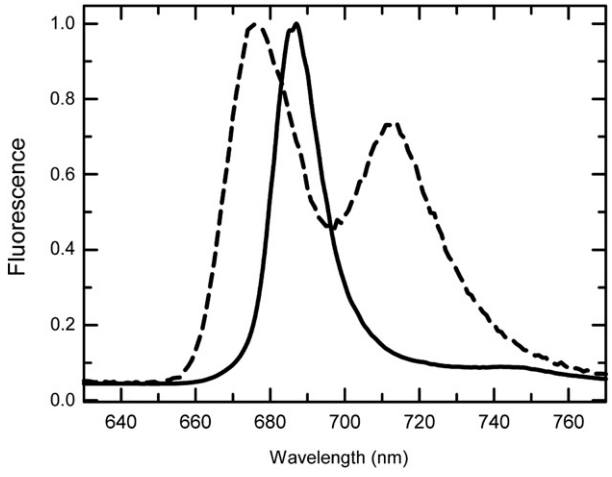

Fig. 2. 77 K fluorescence emission spectra of FCP-like (*solid*) and PSI–LHCr (dashed) zone of sucrose density gradient. The excitation wavelength was 435 nm; spectra are normalized to their maxima.

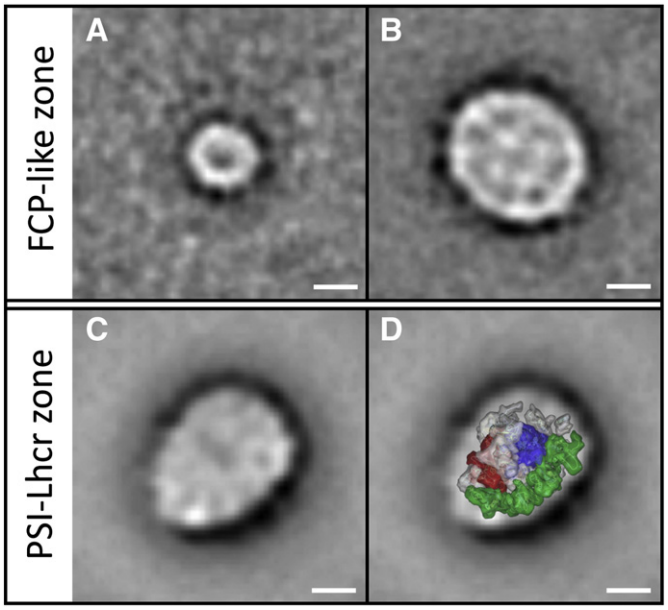

Fig. 3. Single particle analysis of top-view projection maps of *C. velia* photosynthetic pigment–protein complexes. A), B) Representation of the subunit organization in FCP-like zone isolated from *C. velia* obtained by classification of 6400 particles. The most representative class averages of top-view projections of (A) trimeric FCP-like complex; (B) oligomeric FCP-like complex. C), D) Schematic representation of the overall structure of the most representative top-view PSI–LHCr complex projection map of negatively stained particles from sucrose density gradient PSI–LHCr zone. The projections are overlaid with an improved model of plant PSI core complex (blue-PsaA, red-PsaB, gray-small subunits) and green coloured LHC antennae (PDB ID: 2WSF) [42]. The coordinates are taken from Protein Data Bank (http://www.rcsb.org/pdb) [51]. (C) Plain and (D) with model code 2WSF. The scale bar represents 5 nm.

[34]. In order to test whether the apparent similarity of supramolecular organization of the antenna complexes visible in the electron microscopy images reflects the similarity of pigment–protein interactions within these antennae, circular dichroism (CD) spectroscopy was employed.

For CD spectra measurements, samples of *C. velia* antenna were prepared by gel filtration from the second zone of the sucrose density gradient to separate complexes of different sizes [Supplementary Fig. 5a]. Fig. 4 shows a representative absorbance and CD spectrum of a *C. velia* antenna complex. The CD spectrum had positive peaks at 662 nm, 545 nm, 445 nm and 407 nm, negative peaks were observed at 680 nm, 465 nm and 435 nm. These bands were present in spectra of all the gel-filtration fractions with the exception of the positive band at 662 nm, which was highest in the early eluting fractions, gradually decreased in amplitude and was absent in the late fractions i.e. smallest particles [Supplementary Fig. 5b]. This suggests that this feature originates from the interactions related to the formation of oligomeric states. Moreover, the later fraction contained lower amount of isofucoxanthin-like carotenoid compared to violaxanthin and Chl *a*. These fractions most probably represent monomeric complexes originating from the disintegration of trimers and oligomers. Changes in the carotenoid composition accompanying changes in the aggregation state were previously observed in FCP complexes [29].

Comparison of the CD and the absorbance spectrum indicated that the conspicuous positive peak around 545 nm was due to the long-absorbing isofucoxanthin-like carotenoid.

Fig. 4 also presents the absorbance and CD spectrum of an XLH complex from *X. debile*. Isolation of this complex and its detailed spectroscopic analysis were described recently [34,35]. The CD of the XLH complex of *X. debile* matches the spectrum of antenna complexes from another representative of xanthophytes, *Pleurochloris meiringensis* measured earlier by Büchel and Garab [36]. Comparison of the FCP-like and XLH complexes (Fig. 4) shows excellent correspondence throughout the whole range of the spectrum, with the exception of the peak around 660 nm. The difference in the position of the positive feature in the

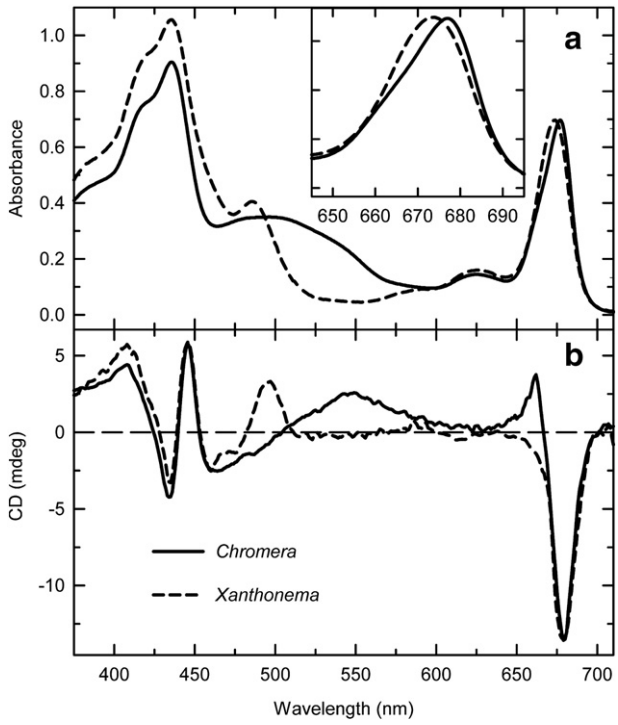

Fig. 4. Absorbance (a) and circular dichroism (b) spectra of the FCP-like antenna complexes of *Chromera velia* (solid line) and *Xanthonema debile* (dashed line).

carotenoid region (545 nm in *Chromera* vs 495 nm in *Xanthonema*) can be easily explained by differences in carotenoid composition between these species, which is also obvious from comparison of the absorbance spectra, namely the lack of carotenoids absorbing above 530 nm in *X. debile* [34]. Hence the only major difference is found in the Q_y region of the absorption spectrum. The positive peak at 662 nm present in the *C. velia* complex is absent from the spectra of antenna of both *X. debile* and *P. meiringensis*. Closer comparison of the absorbance spectra (inset in Fig. 4) in the Qy region shows that the absorption maximum of the *C. velia* FCP-like complex is red-shifted by about 4 nm with respect to the XLH and that there is a pronounced shoulder around 665 nm. This suggests that the transition around 665 nm is also responsible for the presence of the positive feature in the CD spectrum.

It is worth mentioning here that the CD spectra of antenna complexes from *C. velia* and xanthophytes are very different from FCP [e.g. 25,29], LHCII [e.g. 37] and LHCI [38] available in literature, despite the assumed similarity of 3D structures of these complexes that all belong to the large LHC family.

The recent phylogenetic analysis of the LHC proteins from *C. velia* did indicate similarity between some of their genes and xanthophytes' LHC [11]. However, the sample analyzed in the cited work lacked a representative data of xanthophyte antenna proteins, which comprised just two sequences from *V. litorea* (Lhc1 and Lhc3) out of total of about 600 of sequence analyzed. The present results support the similarity of the FCP-like LHCs from chromerids and xanthophytes as well.

In the present work, no indications of association of FCP-like antenna with photosystems in *C. velia* were observed, compared to some other organisms [27,39,40, etc.]. Interestingly, similar uncoupling was observed also in the *X. debile* [34], an organism with FCP-like antennae closely related to *C. velia*.

The unique properties of the antenna complex in *C. velia* surely justify a proposition of a label, CLH, for "Chromera Light Harvesting" complex. This is analogous to the abbreviation XLH, that was applied to the antenna complex of *Xanthonema* previously [34]. This labeling i) emphasizes the spectroscopic and structural features shared between chromerids and xanthophytes; ii) avoids using pigment composition for the basis of the indefinite naming convention and iii) differentiates the [species] LH proteins from the canonical FCP proteins of diatoms.

3.2. PSI–LHCr zone

SDS-PAGE electrophoresis of the PSI–LHCr (fourth) zone showed a band with apparent mass of about 65–70 kDa, characteristic for the PsaB protein of PSI complex [40]. The two bands with apparent weights of about 25 and 45 kDa were confirmed by mass spectrometry as PsaA-1 and PsaA-2 subunits of PsaA protein (R. Sobotka, J. Lukes and P. Keeling, personal communication).

The identification of PsaA-1, -2 subunits is supported by analysis of *C. velia* chloroplast genome [48] which shows that the PsaA is split into two genes, denoted as *psaA-1* (909 basepairs, 302 amino acids, theoretical molecular weight of gene product 32 kDa) and *psaA-2* (1299 basepairs, 432 amino acids, theoretical molecular weight of gene product 49 kDa). These are separated by a 5.5 kb section in which 4 protein-coding genes were predicted, including the gene for the photosystem II CP 47 subunit, *psbB*. This splitting of the protein for a component of the photosystem I core appears to be a unique property of *C. velia*.

A BLASTp® [49] search was performed on protein sequences derived from the available transcriptome sequence and genome sequence from *C. velia* and transcriptome sequence data for PsaA-1 and PsaA-2. These results showed that whilst both sequences corresponded to portions of the PsaA protein of PSI, they differed markedly in amino acid sequence identity to known genes for the PSI RC subunit, PsaA, from cyanobacteria, dinoflagellates, heterokonts, red and green algae and plants. In all comparisons, the observed identities ranged between 20–40%, and 50–70% with up to 95% coverage for PsaA-1 and PsaA-2, respectively.

The number and position of the transmembrane helices in the structure of both *C. velia* PsaA protein subunits were predicted using the online TMPred tool [50], and compared to the PsaA protein from plant and cyanobacterial PSI [41–43]. Analysis indicated four transmembrane domains in the PsaA-1 protein and seven in the PsaA-2 [Supplementary Fig. 6a]. By putting these subunits together, it is possible to form the expected eleven-helix structure of photosystem I core subunit. Moreover, these results strongly suggest that the split in the *psaA* gene in *C. velia* occurred between the helix IV and V (according to the numbering used by Schubert et al. [41] [Supplementary Fig. 6b]), that is within the domain that fulfils the light harvesting function and that does not follow the boundary between the antenna and core domain of the PsaA protein [41]. Detailed phylogenetic analysis of the sequences of components of the PSI in *C. velia* is beyond the intended scope of this paper but the present results suggest that such analysis might yield a plethora of interesting insights into phylogenetic, structural and functional aspects of photosystem I.

The SDS-PAGE of the PSI–LHCr zone showed also a marked band with a mass of about 30 kDa (Fig. 1) which corresponds to a LHC-family protein [44], clearly different from the CLH (see above) antenna proteins of the FCP-like zone. Mass spectrometry of this band identified a "Putative fucoxanthin chlorophyll a/c protein (CveliaI_13309.t1, Supplementary data 2.b)" with 11 identified out of 22 possible peptides, sequence coverage 46.2%. BLASTp was performed to confirm the relatedness of this sequence to red alga LHC family proteins. The data indicated, that the PSI–LHCr zone (zone 4) contains the PSI complexes with antennae similar to the LHCr, red alga-like LHC [11,44,45]. Comparison with the work of Pan et al. [11] showed that our LHCr protein is not present in their dataset. However, these authors identified several *C. velia* genes similar to LHCr and further analysis confirmed that our sequence belonged to the same group of proteins (not shown).

The fluorescence emission spectrum at 77 K of PSI–LHCr zone (Fig. 2) had maxima at 676 and 714 nm. The longwave emission at 714 nm

probably originates in the red chlorophyll states within the PSI complex as has been previously observed in diatoms PSI [27]. The peak at 676 nm indicates the presence of LHCr complexes uncoupled from the PSI core complex, although we were not able to identify any free LHCr monomers in the TEM images. A fluorescence emission spectrum of PSI–LHCr zone very close to that shown in Fig. 2 was observed earlier in samples isolated from a red-alga *Cyanidium caldarium* [45].

The purified PSI–LHCr complexes were visualized by electron microscopy and a quantity of 4200 particles from 40 micrographs [Supplementary Fig. 4b] were selected to perform the image analysis. After the classification steps, selected PSI–LHCr complexes were divided into 5 classes. The averaged top-view projections of all classes had an oval shape with no apparent symmetry. The class averages represent monomeric PSI particles with small stain heterogeneity at the edge of the complexes, as shown previously in green algae and higher plants [46,47]. The most representative class average of the PSI–LHCr complexes is shown in Fig. 3C–D. The particle can be overlaid with a projection of X-ray structure of plant PSI–LHCI supercomplex containing PsaA/B heterodimer and a row of four LHCI subunits [43]. Similar particles which demonstrate PSI core complexes with bound LHCI-type light harvesting antenna were observed previously in green and red algae [44,45]. The results indicate that the PSI RC from *C. velia* appears to form a regular photosystem I structure.

3.3. Conclusions

In summary, when grown in natural light conditions, *C. velia* uses two types of light harvesting antennae systems, each related to light harvesting complexes from different phylogenetic groups of photosynthetic organisms. One type of antenna, the CLH, shows pigments and proteins similar to FCP complexes, however, the single particle analysis and spectroscopic data suggested its close relation to antenna from xanthophytes. *C. velia* also contains a PSI-bound LHCr complex, related to the LHCI proteins of red algae, which makes *C. velia* an interesting organism that utilizes two different and evolutionary distant types of light harvesting complexes.

Acknowledgements

This research was supported by the GAAV 32-IAA601410907 and GAJU 134/2010/P with institutional support RVO:60077344. Research on *C. velia* genomics is supported by an Award IC/2010/09 made by the King Abdullah University of Science and Technology (KAUST) to A. Pain. The authors are greatly indebted to the team of J. Lukes, R. Sobotka and P. Keeling, for giving access to their data concerning the split of the photosystem I reaction center protein prior to publication. Thanks are extended to I. Hunalova and F. Matousek for technical assistance.

Appendix A. Supplementary data

Supplementary data to this article can be found online at http://dx.doi.org/10.1016/j.bbabio.2013.02.002.

References

[1] R.B. Moore, M. Obornik, J. Janouskovec, T. Chrudimsky, M. Vancova, D.H. Green, S.W. Wright, N.W. Davies, C.J.S. Bolch, K. Heimann, J. Slapeta, O. Hoegh-Guldberg, J.M. Logsdon Jr., D.A. Carter, A photosynthetic alveolate closely related to apicomplexan parasites, Nature 451 (2008) 959–963.
[2] M. Obornik, D. Modry, M. Lukes, E. Cernotikova-Stribrna, J. Cihlar, M. Tesarova, E. Kotabova, M. Vancova, O. Prasil, J. Lukes, Morphology, ultrastructure and life cycle of Vitrella brassicaformis n. sp., n. gen., a novel Chromerid from the Great Barrier Reef, Protist 163 (2012) 306–323.
[3] L. Lim, G.I. McFadden, The evolution, metabolism and functions of the apicoplast, Phil. Trans. R. Soc. B 365 (2010) 749–763.
[4] T. Cavalier-Smith, Principles of protein and lipid targeting in secondary symbiogenesis: Euglenoid, Dinoflagellate, and Sporozoan plastid origins and the eukaryote family tree, J. Eukaryot. Microbiol. 46 (1999) 347–366.
[5] J.M. Archibald, The puzzle of plastid evolution, Curr. Biol. 19 (2009) 81–88.
[6] B.R. Green, After the primary endosymbiosis: an update on the chromalveolate hypothesis and the origins of algae with Chl *c*, Photosynth. Res. 107 (2011) 103–115.
[7] M. Obornik, M. Vancova, D.H. Lai, J. Janouskovec, P.J. Keeling, J. Lukes, Morphology and ultrastructure of multiple life cycle stages of the photosynthetic relative of Apicomplexa, *Chromera velia*, Protist 162 (2011) 115–130.
[8] E. Kotabova, R. Kana, J. Jaresova, O. Prasil, Non-photochemical fluorescence quenching in *Chromera velia* is enabled by fast violaxanthin de-epoxidation, FEBS Lett. 585 (2011) 1941–1945.
[9] S. Fietz, W. Bleiβ, D. Hepperle, H. Koppitz, L. Krienitz, A. Nicklisch, First record of *Nannochloropsis limnetica* (Eustigmatophyceae) in the autotrophic picoplankton from Lake Baikal, J. Phycol. 41 (2005) 780–790.
[10] J. Janouskovec, A. Horak, M. Obornik, J. Lukes, P.J. Keeling, A common red algal origin of the apicomplexan, dinoflagellate, and heterokont plastids, Proc. Natl. Acad. Sci. U.S.A. 107 (2010) 10949–10954.
[11] H. Pan, J. Slapeta, D. Carter, M. Chen, Phylogenetic analysis of the light-harvesting system in *Chromera velia*, Photosynth. Res. 111 (2012) 19–28.
[12] B. Lepetit, D. Volke, M. Gilbert, C. Wilhelm, R. Goss, Evidence for the existence of one antenna-associated, lipid-dissolved and two protein-bound pools of diadinoxanthin cycle pigments in diatoms, Plant Physiol. 154 (2010) 1905–1920.
[13] J.A.D. Neilson, D.G. Durnford, Structural and functional diversification of the light-harvesting complexes in photosynthetic eucaryotes, Photosynth. Res. 106 (2010) 57–71.
[14] R.R. Guillard, J.H. Ryther, Studies of marine planktonic diatoms I. *Cyclotella nana Hustedt* and *Detonula confervacea* (cleve) gran, Can. J. Microbiol. 8 (1962) 229–239.
[15] K.H. Lichtenthaler, Chlorophylls and carotenoids: pigments of photosynthetic biomembranes, Methods Enzymol. 148 (1987) 350–385.
[16] R.J. Porra, The chequered history of the development and use of simultaneous equation for the accurate determination of chlorophylls *a* and *b*, Photosynth. Res. 73 (2002) 149–156.
[17] S.W. Jeffrey, J.M. LeRoi, Phytoplankton pigments in oceanography, in: S.W. Jeffrey, R.F.C. Mantoura, S.W. Wright (Eds.), Monographs on Oceanographic Methodology 10, UNESCO, France, 1997, pp. 181–205.
[18] J. Frank, M. Radermacher, P. Penczek, J. Zhu, Y.H. Li, M. Ladjadj, A. Leith, SPIDER and WEB: processing and visualization of images in 3D electron microscopy and related fields, J. Struct. Biol. 116 (1996) 190–199.
[19] M. van Heel, J. Frank, Use of multivariate statistics in analyzing the images of biological macromolecules, Ultramicroscopy 6 (1981) 187–194.
[20] G. Harauz, E.J. Boekema, M. van Heel, Statistical image analysis of electron micrographs of ribosomal subunits, Methods Enzymol. 164 (1988) 35–49.
[21] C. Woehle, T. Dagan, W.F. Martin, S.B. Gould, Red and problematic green phylogenetic signals among thousands of nuclear genes from the photosynthetic and apicomplexa-related *Chromera velia*, Genome Biol. Evol. 3 (2011) 1220–1230.
[22] S.F. Altschul, T.L. Madden, A.A. Schäffer, J. Zhang, Z. Zhang, W. Miller, D.J. Lipman, Gapped BLAST and PSI-BLAST: a new generation of protein database search programs, Nucleic Acids Res. 25 (1997) 3389–3402.
[23] M. Eppard, E. Rhiel, The genes encoding light-harvesting subunits of *Cyclotella cryptica* (*Bacillariophyceae*) constitute a complex and heterogeneous family, Mol. Gen. Genet. 260 (1998) 335–345.
[24] A. Beer, K. Gundermann, J. Beckmann, C. Büchel, Subunit composition and pigmentation of fucoxanthin-chlorophyll proteins in diatoms: evidence for a subunit involved in diadinoxanthin and diatoxanthin binding, Biochemistry 45 (2006) 13046–13053.
[25] B. Lepetit, D. Volke, M. Szabo, R. Hoffmann, G. Garab, C. Wilhelm, R. Goss, Spectroscopic and molecular characterization of the oligomeric antenna of the diatom *Phaeodactylum tricornutum*, Biochemistry 46 (2007) 9813–9822.
[26] T. Veith, J. Brauns, W. Weisheit, M. Mittag, C. Büchel, Identification of a specific fucoxanthin-chlorophyll protein in light harvesting complex of photosystem I in diatom *Cyclotella meneghiniana*, Biochim. Biophys. Acta 1787 (2009) 905–912.
[27] Y. Ikeda, M. Komura, M. Watanabe, C. Minami, H. Koike, S. Itoh, Y. Kashino, K. Satoh, Photosystem I complexes associated with fucoxanthin-chlorophyll-binding proteins from a marine centric diatom *Chaetoceros gracilis*, Biochim. Biophys. Acta 1777 (2008) 351–361.
[28] E. Papagiannakis, I.H.M. van Stokkum, H. Fey, C. Büchel, R. van Grondelle, Spectroscopic characterisation of the excitation energy transfer in the fucoxanthin-chlorophyll protein of diatoms, Photosynth. Res. 86 (2005) 241–250.
[29] C. Büchel, Fucoxanthin-chlorophyll proteins in diatoms: 18 and 19 kDa subunits assemble into different oligomeric states, Biochemistry 42 (2003) 13027–13034.
[30] G.F. Peter, J.P. Thornber, Biochemical composition and organization of higher plant photosystem II light-harvesting pigment–proteins, J. Biol. Chem. 266 (1991) 16745–16754.
[31] J.P. Dekker, H. van Roon, E.J. Boekema, Heptameric association of light-harvesting complex II trimers in partially solubilized photosystem II membranes, FEBS Lett. 449 (1999) 211–214.
[32] W. Kühlbrandt, D.N. Wang, Y. Fujiyoshi, Atomic model of plant light-harvesting complex by electron crystallography, Nature 367 (1994) 614–621.
[33] J. Standfuss, A.C.T. van Scheltinga, M. Lamborghini, W. Kühlbrandt, Mechanisms of photoprotection and nonphotochemical quenching in pea light-harvesting complex at 2.5 Å resolution, EMBO J. 24 (2005) 919–928.
[34] Z. Gardian, J. Tichy, F. Vacha, Structure of PSI, PSII and antennae complexes from yellow-green alga *Xanthonema debile*, Photosynth. Res. 108 (2011) 25–31.
[35] M. Durchan, J. Tichy, R. Litvin, V. Slouf, Z. Gardian, P. Hribek, F. Vacha, T. Polivka, Role of carotenoids in light-harvesting processes in an antenna protein from the chromophyte *Xanthonema debile*, J. Phys. Chem. B 116 (2012) 8880–8889.
[36] C. Büchel, G. Garab, Organization of the pigment molecules in the chlorophyll a/c light-harvesting complex of *Pleurochloris meiringensis* (xanthophyceae).

Characterization with circular dichroism and absorbance spectroscopy, J. Photochem. Photobiol. B Biol. 37 (1997) 118–124.
[37] A.V. Ruban, F. Calkoen, S.L.S. Kwa, R. van Grondelle, P. Horton, J.P. Dekker, Characterisation of LHC II in the aggregated state by linear and circular dichroism spectroscopy, Biochim. Biophys. Acta Bioenerg. 1321 (1997) 61–70.
[38] V.H.R. Schmid, K.V. Cammarata, B.U. Bruns, G.W. Schmidt, In vitro reconstitution of the photosystem I light-harvesting complex LHCI-730: heterodimerization is required for antenna pigment organization, Proc. Natl. Acad. Sci. U.S.A. 94 (1997) 7667–7672.
[39] T. Brakemann, W. Schlörmann, J. Marwuardt, M. Nolte, E. Rhiel, Association of fucoxanthin chlorophyll a/c-binding polypeptides with photosystems and phosphorylation in the centric diatom *Cyclotella cryptica*, Protist 157 (2006) 463–475.
[40] T. Veith, C. Büchel, The monomeric photosystem I-complex of the diatom *Phaeodactylum tricornutum* binds specific fucoxanthin chlorophyll proteins (FCPs) as light-harvesting complexes, Biochim. Biophys. Acta Bioenerg. 1767 (2007) 1428–1435.
[41] W.D. Schubert, O. Klukas, N. Krauss, W. Saenger, P. Fromme, H.T. Witt, Photosystem I of *Synechococcus elongatus* at 4 Å resolution: comprehensive structure analysis, J. Mol. Biol. 272 (1997) 741–769.
[42] P. Jordan, P. Fromme, H.T. Witt, O. Klukas, W. Saenger, N. Krauss, Three-dimensional structure of cyanobacterial photosystem I at 2.5 Å resolution, Nature 411 (2001) 909–917.
[43] A. Amunts, H. Toporik, A. Borovikova, N. Nelson, Structure determination and improved model of plant photosystem I, J. Biol. Chem. 285 (2010) 3478–3486.
[44] J. Kargul, J. Nield, J. Barbes, Three-dimensional reconstruction of a light-harvesting complx I-photosystem I (LHCI-PSI) supercomplex from the green alga *Chlamydomonas reinhardtii*, J. Biol. Chem. 278 (2003) 16135–16141.
[45] Z. Gardian, L. Bumba, A. Schrofel, M. Herbstova, J. Nebesarova, F. Vacha, Organisation of Photosystem I and Photosystem II in red alga Cyanidium caldarium: encounter of cyanobacterial and higher plant concepts, Biochim. Biophys. Acta 1767 (2007) 725–731.
[46] E.J. Boekema, P.E. Jensen, E. Schlodder, J.F.L. van Breemen, H. van Roon, V.H. Scheller, J.P. Dekker, Green plant photosystem I binds light-harvesting complex I on one side of the complex, Biochemistry 40 (2001) 1029–1036.
[47] M. Germano, A.E. Yakushevska, W. Keegstra, H.J. van Gorkom, J.P. Dekker, E.J. Boekema, Supramolecular organization of photosystem I and light-harvesting complex I in *Chlamydomonas reinhardtii*, FEBS Lett. 525 (2002) 121–125.
[48] NCBI reference sequence NC_014340.1, http://www.ncbi.nlm.nih.gov/genome/genomes/12053?subset=organelles&details=on&, (08. 20. 2012).
[49] http://www.ncbi.nlm.nih.gov/blast, (08. 20. 2012, the basic local alignment search tool BLAST).
[50] http://www.ch.embnet.org/software/TMPRED_form.html, (08. 20. 2012, TMPred tool).
[51] http://www.rcsb.org/pdb, (08. 20. 2012, RSCB protein data bank).